



Ab initio study of the *fcc*-WC(1 0 0) surface and its interaction with cobalt monolayers

V.G. Zavodinsky*

Institute of Materials of Khabarovsk Scientific Centre of Far Eastern Branch of the Russian Academy of Sciences, 153 Tikhokeanskaya str., Khabarovsk, 680042, Russia

ARTICLE INFO

Article history:

Received 1 September 2010
Received in revised form
11 November 2010
Accepted 11 November 2010
Available online 19 November 2010

Keywords:

Tungsten carbide
WC(1 0 0) surface
Cobalt monolayer
Ab initio calculations

ABSTRACT

The WC(1 0 0) surface has been studied by using ab initio methods of the density functional theory and pseudopotentials. Calculations have shown that surface and undersurface atoms move from their bulk positions. Namely, carbon atoms moved outward, while tungsten atoms moved inward. Five geometric cases for Co/WC(1 0 0) system were compared: (A) Co atoms are above C atoms; (B) Co atoms are above W atoms; (C) Co atoms are in the four-fold sites above WC pairs; (D and E) Co atoms are above the W–W–C and C–C–W three-fold sites, respectively – and the (A) case has been found to be energetically preferable. In all cases, Co layers have been found to be ferromagnetic. The densities of states for the bulk *fcc*-WC, the WC(1 0 0) surface, and the WC/Co system were compared.

© 2010 Elsevier B.V. All rights reserved.

1. Introduction

Bulk cubic WC phase is unstable at room temperatures, therefore there are only a few theoretical works devoted to studying its properties. Price and Cooper [1] have calculated the equilibrium lattice constant, the bulk modulus and the bulk density of states; Hugosson et al. [2] have reported the calculated surface energy and the work function for the WC(1 0 0) surface; Vojvodic et al. [3] have studied the adsorption properties and electronic states of the WC(1 1 1) surface; Vines et al. [4] have discussed the reasons of instability of cubic-WC; Ilyasov et al. [5] have modeled the WC–Fe–Ni hard materials based on cubic WC; Christensen et al. [6] have used cubic WC as a model for studying the interaction of WC with cobalt. Meanwhile, a significant part of WC nanocrystallites included in advanced Co-cemented hard alloys demonstrates a cubic symmetry [7–10]. Moreover, recent ab initio calculations [11] have demonstrated that the atomic structure of the WC trigonal nanocrystallites has much in common with the structure of cubic crystallites. Namely, boundaries of both types of particles contain W and C atoms in the NaCl-like manner. Besides, it was concluded in Ref. [3] that the (1 0 0) surfaces of transition-metal carbides are more energetically stable than the (1 1 1) ones. However, even nowadays there is no detailed information on the atomic structure (relaxation effects) and electronic states of the

WC(1 0 0) surface. Thus, the investigation of the WC(1 0 0) surface is timely and important for nanostructured materials applications.

Knowledge of atomic structure and energetics of the WC/Co interface is a keystone for understanding the properties of hard alloys especially for the cases when the sizes of WC crystallites aspire to 50–100 nm and the thickness of Co interlayers falls to 1–2 nm. The smallest observed particles, 300–500 nm in size, are characterized by trigonal or cubic shapes [7–10] with very sharp interfaces (not thicker than 1–2 nm). Quantitative analysis of WC/Co interface for *hex*-WC crystal boundaries was performed in some works [6,9,12–15], however, there is lack of information on the structure of the Co boundary with the *fcc*-cubic WC. Energetics and electronic states of the WC(1 0 0)/Co interface were studied by Christensen et al. [6], however, the authors considered only periodically layered WC/Co systems without free surfaces, and besides, ignored the ferromagnetism of cobalt.

Therefore, the goal of the present work is to study a clean WC(1 0 0) surface and a monolayer of cobalt placed on a free WC(1 0 0) surface taking into account spin-polarization effects. Though we assumed to use our results for particles, we regarded the surface of an unlimited crystal as a surface of a particle of some tens or hundreds nanometers in size.

2. Methods and approaches

All calculations were performed within the framework of the density functional theory (DFT) [16,17] using the plane wave basis

* Corresponding author. Tel.: +7 4212 226956; fax: +7 4212 226598.
E-mail address: vzavod@mail.ru

set, the generalized gradient approximation (GGA) [18], and the pseudopotential method [19], as implemented in a spin-polarized version of the FHI96md package [20].

Pseudo-potentials for carbon and tungsten used were the same as utilized in Ref.11. They were generated through the FHI98PP package [21] and were tested to describe lattice constants and bulk elastic modules for WC, both the hexagonal and cubic phases. The pseudopotential for cobalt has been constructed with the following parameters: $r_s = 1.15 \text{ \AA}$, $r_p = 1.54 \text{ \AA}$, $r_d = 1.15 \text{ \AA}$, $r_{\text{core}} = 0.53 \text{ \AA}$. Here r_s , r_p , and r_d are the cutoff radii for s -, p -, and d -components and r_{core} is the radius of the nonlinear core-valence correction. The Co pseudopotential, calculated in the scheme of Troullier–Martins [22], was checked for the absence of ‘ghost’ states. Then it was tested for determining the equilibrium lattice parameter a_0 , the magnetic moment M and the bulk elastic modulus B for the bulk fcc-Co . The values of a_0 and B were found using the Murnaghan equation of state [23]. The calculated values of the total energy versus the cell volume, E_{tot} (V), are plotted in Fig. 1

Calculated equilibrium values for bulk fcc-Co ($a_0 = 3.62 \text{ \AA}$, $B = 205 \text{ GPa}$, and $M = 1.75 \mu_B$) are close to experimental ones [24] (3.54 \AA , 191 GPa , and $1.72 \mu_B$). For these calculations the 6 k -points of the Brillouin zone (Γ -point (0,0,0) with a $2 \times 2 \times 2$ grid as proposed by the Monkhorst–Pack scheme [25]) were used with the kinetic energy cutoff of 680 eV. For comparison, the $3 \times 3 \times 3$ Monkhorst–Pack scheme with 18 k -points leads to $a_0 = 3.60 \text{ \AA}$, $B = 212 \text{ GPa}$, and $M = 1.65 \mu_B$.

In order to investigate Co layers on the WC(100) surface we used a periodic WC slab consisting of seven WC layers with two WC pairs in each layer. The planar 1×1 periodicity of the slab corresponded to the calculated equilibrium fcc-WC lattice with the $a_0 = 4.39 \text{ \AA}$ [11]. (The experimental value is equal to $4.22\text{--}4.27 \text{ \AA}$ (see citations in Ref. [6]). To eliminate possible artificial asymmetric effects, cobalt layers were placed simultaneously on both surfaces of the slab. One of the sides of the slab is presented in Fig. 2 together with the adsorbed Co atoms. The empty space between the WC/Co slab systems was established at approximately one nanometer. In the majority of the cases the WC-Co calculations were implemented with the number of k -points of 9 (the $3 \times 3 \times 1$ Monkhorst–Pack scheme) with the energy cutoff of 680 eV, but in special tests the number of k -points has increased to 28. Special tests included studying the sensitivity of results to the slab thick-

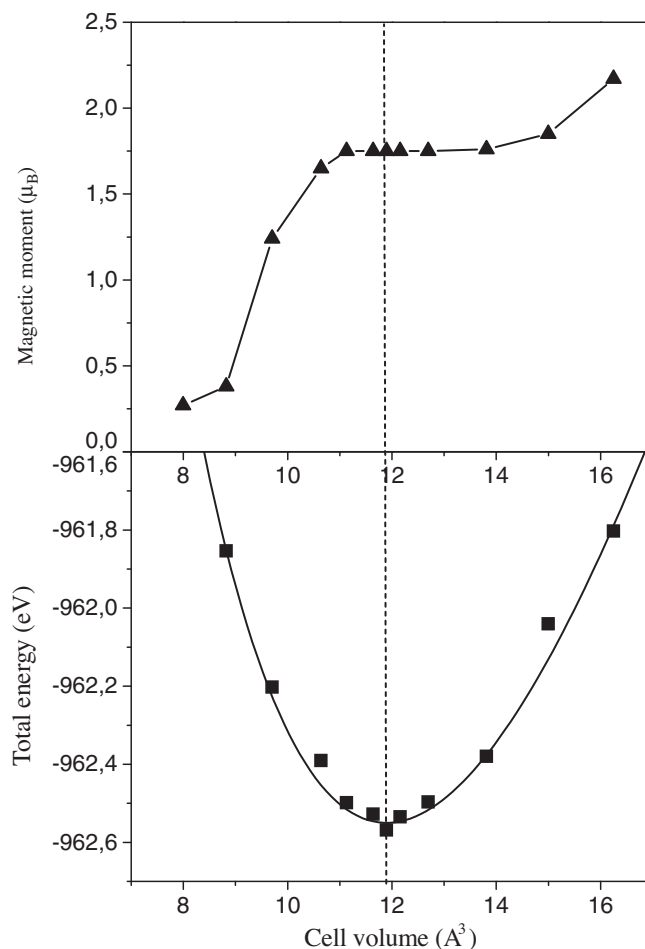


Fig. 1. Total energy E_{tot} (V) (low panel) and magnetic moment M (top panel) for fcc-Co as a function of the cell volume V . Black squares are calculated points; the solid curve in the low panel is obtained following the Murnaghan equation. Vertical dotted line indicates the equilibrium volume value.

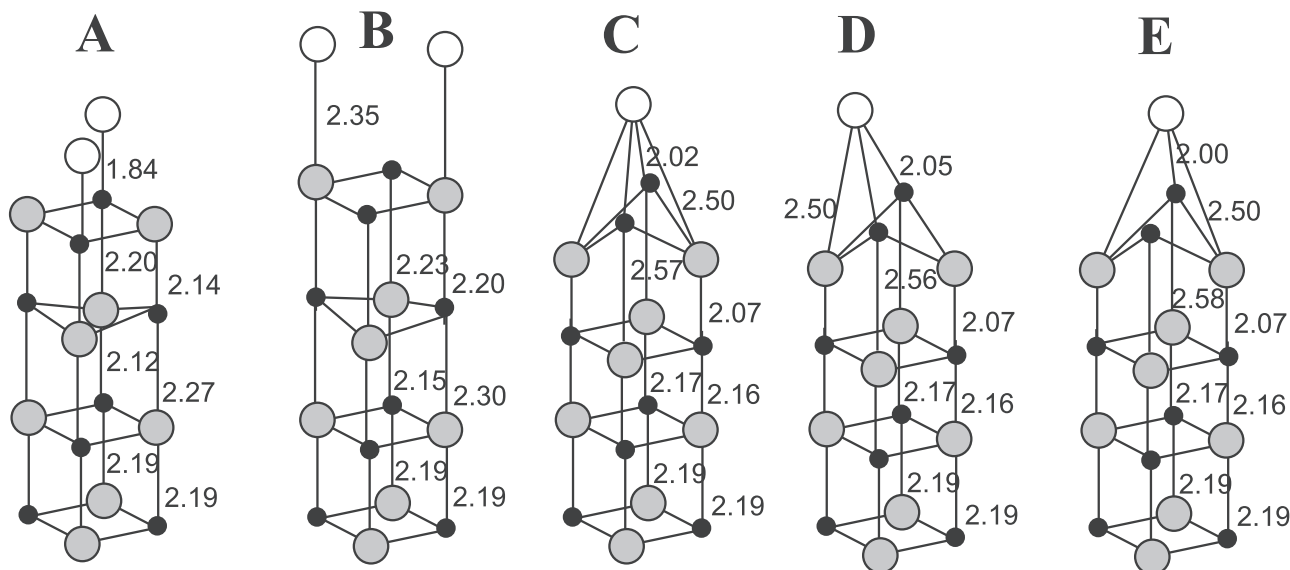


Fig. 2. Atomic scheme of WC slab with WC(100) surfaces. A, B, C, D, and E are the different configurations in which atoms of the Co monolayer were placed. Gray circles are W atoms, black ones are C atoms, and white circles represent Co atoms.

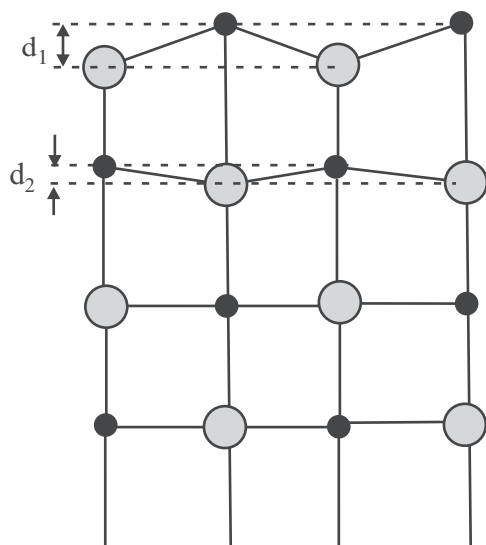


Fig. 3. Vertical (d_1) and subsurface (d_2) separations of W and C atoms at the free WC(100) surface.

ness and to the energy cutoff. Only two WC layers (surface and undersurface) were relaxed, but internal layers of the slab were kept in their bulk positions. The self-consistency convergence was provided by stabilization of the total energy with an accuracy of 0.005 eV per atom. Electron densities of states were represented by superpositions of the Gaussian functions centered on each electron level.

3. Results and discussions

3.1. Clean WC(100) surface

The first task of this work was to study the clean WC(100) surface. Calculations have shown that surface and undersurface atoms moved from their bulk positions. Namely, carbon atoms moved outward, while tungsten atoms moved inward. Vines et al. [4] observed the same behavior of the (100) surface in the case of cubic carbides of some transition metals (MeC) and reported the values of the vertical Me–C separations ($d_1 = 0.09\text{--}0.25 \text{ \AA}$ for the surface layer and $d_2 = 0.04\text{--}0.08 \text{ \AA}$ for the undersurface layer, dependently on metal), however, they did not provide such calculations for WC. Our calculations show $d_1 = 0.30 \text{ \AA}$ and $d_2 = 0.06 \text{ \AA}$ (Fig. 3).

By comparing the total energies of bulk crystal (E_{bulk}) and of the slab (E_{slab}) it is possible to find the surface energy E_{surf} :

$$E_{\text{surf}} = \frac{(E_{\text{slab}}(N) - E_{\text{bulk}}(N))}{2S}$$

where N symbolizes that E_{bulk} and the E_{slab} correspond to the same number N of WC pairs, S is the one-side surface square of the slab.

Our calculations estimate the WC(100) surface energy at 2.14 J/m^2 . The known reported values are 2.64 J/m^2 for the relaxed surface [2] and 1.6 J/m^2 for unrelaxed [12].

This study does not apply to detailed research of electronic structure of the WC(100) surface, however, it is interesting to consider and discuss here the density of the surface states. The WC slab, used in this work, contains surface states mixed with bulk-like ones, and it is rather difficult to separate them. However, it is possible to obtain some important information by comparing the densities of states (DOS) of slab and bulk.

The calculated DOS for the WC slab are plotted in Fig. 4 in comparison with the bulk data. The bulk DOS calculations were performed here by using the same cell and k -points as in the slab

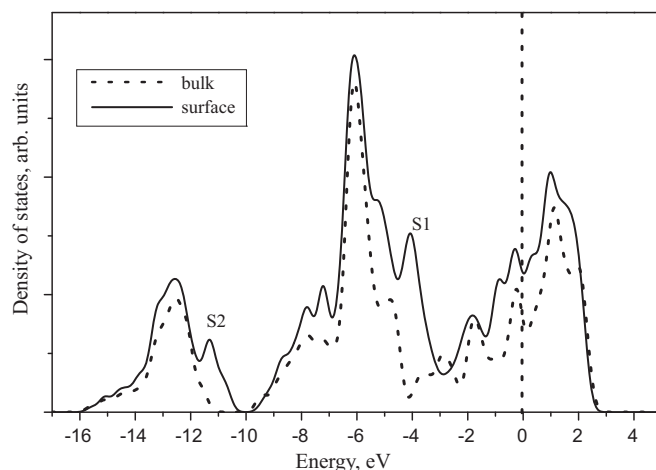


Fig. 4. Densities of states for the tungsten carbide slab with the (100) surface and for the bulk cubic WC. Vertical dotted line shows the Fermi level.

calculations. One can see that the DOS for the slab differs from the DOS for the bulk crystal mainly by two peaks: namely, S1 and S2 at -4 eV and -11 eV under the Fermi level. One can conclude that these peaks may be interpreted as surface peaks.

3.2. Cobalt layers on the WC(100) surface

The Co/WC(100) interface was regarded as a hetero-epitaxial boundary between two *fcc*-structures. As the *fcc*-WC lattice constant ($a_{0\text{calculated}} = 4.39 \text{ \AA}$) is larger than the lattice constant of cobalt ($a_{0\text{calculated}} = 3.62 \text{ \AA}$), the cobalt layers have been stretched to obtain coherent periodic structures. For the one monolayer (1 ML) film five configurations have been studied (see Fig. 2): (A) Co atoms are above C atoms; (B) Co atoms are above W atoms; (C) Co atoms are in the four-fold sites above WC pairs; (D) and (E) Co atoms are above the W–W–C and C–C–W three-fold sites, respectively. Schemes of equilibrium relaxations for the (A), (B), and (C) cases are shown in details in Fig. 5.

One can see that the relaxation of the WC(100) surface in contact with the Co monolayers differs from the relaxation of the free WC(100) surface. In the (A) and (B) cases, the behaviors of W and C atoms of the first surface layer have changed drastically: the carbon atoms moved inward and the tungsten atoms moved outward. In the (C) case, the character of relaxation did not change, but the W–C separation more than doubled.

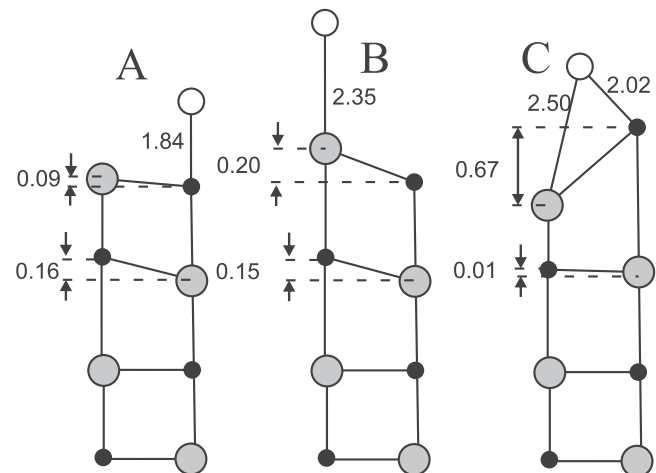


Fig. 5. Schemes of atomic displacements for the WC/Co-1 ML system. Distances are shown in angstroms. Notations A, B, and C are the same as in Fig. 2.

Table 1
The binding E_{bind} and separation E_{sep} energies, the magnetic moment M and the distance d from a Co atom and a surface atom, calculated for the 1 ML Co film on the WC(100) surface. Data of Ref. [6] are presented in brackets.

	Interface configurations				
	A	B	C	D	E
E_{bind} (eV)	4.05	3.04	3.69	3.62	3.64
E_{sep} (J/m ²)	4.18 (4.50)	1.52 (1.58)	3.43	3.31	3.35
d (Å)	1.84 _{Co-C} (1.80)	2.35 _{Co-W} (2.37)	2.02 _{Co-C} ; 2.50 _{Co-W}	2.05 _{Co-C} ; 2.50 _{Co-W}	2.00 _{Co-C} ; 2.50 _{Co-W}
M (μ _B)	1.37	1.55	0.87	1.15	1.22

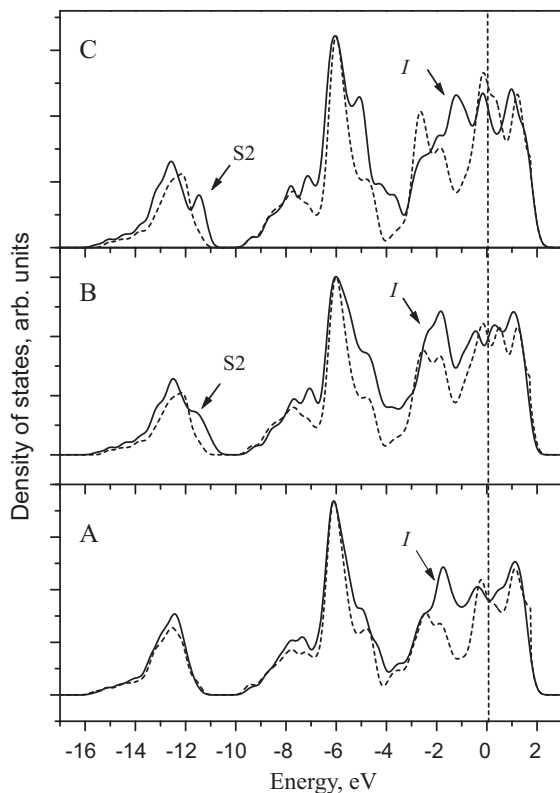


Fig. 6. Densities of states for the Co-1ML contacted with the WC(100) surface. Notations A, B, and C are the same as in Fig. 2. Solid curves represent calculated DOS for the WC/Co-1ML system; dotted curves show the sums of DOS for the bulk WC(100) slab and the free Co layer. Vertical dotted line indicates the Fermi level.

For the energetic characterization of the Co/WC system the binding energy E_{bind} and the separation energy E_{sep} were calculated:

$$E_{\text{bind}} = \frac{E_{\text{tot}} - E_{\text{slab}} - nE_{\text{Co1}}}{n},$$

$$E_{\text{sep}} = \frac{E_{\text{tot}} - E_{\text{slab}} - E_{\text{film}}}{2S},$$

where n is the number of Co atoms, E_{tot} , E_{slab} , E_{Co1} , and E_{film} are, respectively, energies of the Co/WC system, the WC slab, one free Co atom, and the unsupported cobalt film with the geometry corresponding to the relaxed film on the WC surface.

Calculated values of E_{bind} , E_{sep} , the magnetic moment M and the distance d from a Co atom and the nearest surface atom are listed in Table 1.

From these data it is clear that monolayers of cobalt with atoms positioned above carbon atoms are energetically preferable: they have maximal absolute values of the binding and separation energy. As for the magnetic moment, its value does not correlate directly with energy, and further detailed studies are called for. However, it is remarkable that our results for the separation energy and cobalt-surface distances, obtained with the spin-polarization approach,

are close to the corresponding spin-restricted data [6]. This means that spin-restricted calculations can also give correct enough information about the energetics of the WC/Co systems.

The densities of electronic states for the 1 ML cobalt films are plotted in Fig. 6. As it is shown, the shape of the DOS may be on the whole considered the sum of DOSes for the bulk *fcc*-WC and a Co layer. The main visible distinction is the sharp peak I lying at 1.7 eV below the Fermi level. This peak may be interpreted as an interface peak. This peak has the same position as the corresponding peak in the bulk states but its intensity is much larger. In the (B) and (C) cases, the surface peak S2 observed in DOS of the WC(100) slab exists in DOS of the WC/Co systems too.

4. Conclusions

Quantum-mechanics calculations demonstrate that the free WC(100) surface undergoes a relaxation. Namely, carbon atoms move outward, while tungsten atoms move inward. The shape of the density of states for the surface mainly differs from DOS for the bulk crystal by two surface peaks: namely, S1 and S2 at -4 eV and -11 eV under the Fermi level. The monolayers of cobalt with atoms positioned above carbon atoms are energetically preferable. The density of states for the WC/Co-1 ML system looks approximately like the superposition of DOSes for bulk *fcc*-WC and Co monolayers. Co layers are ferromagnetic, however, magnetization does not essentially influence their energetics and geometry.

References

- [1] D.L. Price, B.P. Cooper, Total energies and bonding for crystallographic structures in titanium-carbon and tungsten-carbon systems, *Phys. Rev. B* 39 (1989) 4945–4977.
- [2] H.W. Hugosson, O. Eriksson, U. Jansson, A.V. Ruban, P. Souvatzis, I.A. Abrikosov, Surface energies and work functions of the transition metal carbides, *Surf. Sci.* 557 (2004) 243–254.
- [3] A. Vojvodic, C. Ruberto, B.I. Lundqvist, Atomic and molecular adsorption on transition-metal carbide (111) surfaces from density-functional theory: a trend study of surface electronic factors, *J. Phys.: Condens. Matter* 22 (2010) 375504–375525.
- [4] F. Vines, C. Sousa, P. Liu, J.A. Rodriguez, F. Illas, A systematic density functional theory study of the electronic structure of bulk and (001) surface of transition-metal carbides, *J. Chem. Phys.* 122 (2005) 174709–174719.
- [5] V. Ilyasov, A. Ryzhkin, Y. Ilyasov, Prospects of computer modelling for a level of wear resistance of PM hard materials on the basis WC–Fe–Ni, *Powder Metall. Prog.* 2 (2002) 44–53.
- [6] M. Christensen, S. Dudiy, G. Wahnström, First-principles simulations of metal-ceramic interface adhesion: Co/WC versus Co/TiC, *Phys. Rev. B* 65 (2002) 045408–045415.
- [7] T. Yamamoto, Y. Ikuhara, T. Watanabe, T. Sakuma, Y. Taniuchi, K. Okada, T. Tanase, High resolution microscopy study in Cr₃C₂-doped WC–Co, *J. Mater. Sci.* 34 (2001) 3885–3890.
- [8] C.-S. Kim, G.S. Rohrer, Geometric and crystallographic characterization of WC surfaces and grain boundaries in WC–Co composites, *Interface Sci.* 12 (2004) 19–27.
- [9] M. Christensen, G. Wahnström, C. Alibert, S. Lay, Quantitative analysis of WC grain shape in sintered WC–Co cemented carbides, *Phys. Rev. Lett.* 94 (2005) 066105–066109.
- [10] A. Delanoë, S. Lay, Evolution of the WC grain shape in WC–Co alloys during sintering: effect of C content, *Int. J. Refract. Met. Hard. Mater.* 27 (2009) 140–148.
- [11] V.G. Zavodinsky, Small tungsten carbide nanoparticles: simulation of structure, energetics, and tensile strength, *Int. J. Refract. Met. Hard. Mater.* 28 (2010) 446–450.

- [12] M. Christensen, G. Wahnström, Co-phase penetration of WC(1010)/WC(1010) grain boundaries from first principles, *Phys. Rev. B* 67 (2003) 115415–115425.
- [13] M. Christensen, G. Wahnström, Effects of cobalt intergranular segregation on interface energetics in WC–Co, *Acta Mater.* 52 (2004) 2199–2207.
- [14] G. Östberg, K. Buss, M. Christensen, S. Norgren, H.-O. Andrén, D. Mari, G. Wahnström, I. Reineck, Effect of TaC on plastic deformation of WC–Co and Ti(C,N)–WC–Co, *Int. J. Refract. Met. Hard. Mater.* 24 (2006) 145–154.
- [15] G. Östberg, M.U. Farooq, M. Christensen, H.-O. Andrén, U. Klement, G. Wahnström, Effect of $\Sigma 2$ grain boundaries on plastic deformation of WC–Co cemented carbides, *Mater. Sci. Eng. A* 416 (2006) 119–125.
- [16] H. Hohenberg, W. Kohn, Inhomogeneous electron gas, *Phys. Rev.* 136 (1964) B864–B871.
- [17] W. Kohn, J.L. Sham, Self-consistent equations including exchange and correlation effects, *Phys. Rev.* 140 (1965) A1133–A1138.
- [18] J.P. Perdew, Y. Wang, Accurate and simple density functional for the electronic exchange energy, *Phys. Rev. B* 33 (1986) 8800–8802.
- [19] M.L. Cohen, V. Heine, Pseudopotential theory of cohesion and structure, in: H. Ehrenreich, F. Seitz, D. Turnbull (Eds.), *Solid State Physics*, vol. 24, Academic Press, New York, 1970, pp. 38–249.
- [20] M. Beckstedte, A. Kley, J. Neugebauer, M. Scheffler, Density functional theory calculations for poly-atomic systems: electronic structure, static and elastic properties and ab initio molecular dynamics, *Comp. Phys. Commun.* 107 (1997) 187–205.
- [21] M. Fuchs, M. Scheffler, Ab initio pseudopotentials for electronic structure calculations of poly-atomic systems using density functional theory, *Comp. Phys. Commun.* 119 (1999) 67–165.
- [22] N. Troullier, J.L. Martins, Efficient pseudopotentials for plane-wave calculations, *Phys. Rev. B* 43 (1991) 1993–2006.
- [23] F.D. Murnaghan, The compressibility of media under extreme pressures, *Proc. Natl. Acad. Sci. U.S.A.* 30 (1944) 244–247.
- [24] C. Kittel, *Introduction to Solid State Physics*, 6th ed., Wiley, New York, 1986.
- [25] H.J. Monkhorst, J.D. Pack, Special points for Brillouin-zone integrations, *Phys. Rev. B* 13 (1976) 5188–5192.